

# Viscoelastic and mechanical properties of thermoset PMR-type polyimide–clay nanocomposites

Mohamed O. Abdalla<sup>a</sup>, Derrick Dean<sup>a,\*</sup>, Sandi Campbell<sup>b</sup>

<sup>a</sup>Tuskegee-Center for Advanced Materials, 101 Chappie James Center, Tuskegee University, Tuskegee, AL 36088, USA

<sup>b</sup>NASA Glenn Research Center, Cleveland, OH 44135, USA

Received 1 April 2002; received in revised form 10 July 2002; accepted 15 July 2002

---

## Abstract

High temperature thermoset polyimide–clay nanocomposites were prepared by blending 2.5 and 5 wt% of an unmodified Na<sup>+</sup>-montmorillonite (PGV) and two organically modified PGV (PGVC10COOH, PGVC12) with a methanol solution of PMR-15 precursor. The methanol facilitated the dispersal of the unmodified clay. Dynamic mechanical analysis results showed a significant increase in the thermomechanical properties ( $E'$  and  $E''$ ) of 2.5 wt% clay loaded nanocomposites in comparison with the neat polyimide. Higher glass transition temperatures were observed for 2.5 wt% nanocomposites compared to the neat polyimide. Flexural properties measurements for the 2.5 wt% nanocomposites showed a significant improvement in the modulus and strength, with no loss in elongation. This trend was not observed for the 5 wt% nanocomposites. An improvement in the CTE was observed for the PGV/PMR-15 nanocomposites, while a decrease was observed for the organically modified samples. This was attributed to potential variations in the interface caused by modifier degradation. © 2002 Elsevier Science Ltd. All rights reserved.

**Keywords:** PMR-15; Layered silicates; Nanocomposite

---

## 1. Introduction

The field of polymer–clay hybrids or nanocomposites has attracted considerable attention as a method of enhancing polymer properties and extending their utility, by using molecular or nanoscale reinforcements rather than conventional particulate filled microcomposites [1–13]. Layered silicates (LS) dispersed as a reinforcing phase in a polymer matrix are one of the most important forms of such ‘hybrid inorganic–organic nanocomposites’ [5,6]. The challenge in this area of high performance organic hybrid materials is to obtain significant improvements in the interfacial adhesion between the polymer matrix and the reinforcing material since the organic matrix is relatively incompatible with the inorganic phase. The incompatibility between the organophilic polymer matrix and the hydrophilic-layered silicates has been resolved through chemical substitution on the surface of the clays. As an example, clays of Na<sup>+</sup>-montmorillonite, a natural clay mineral, has been modified to convert the surface from hydrophilic to

organophilic, resulting in clays that are dispersible in common organic solvents [1,2,9,10]. Typically, this is accomplished via a cationic substitution reaction with the surface sodium ion with organics producing organically modified layered silicates (OLS). Within the field of polyimide (PI) based nanocomposites, several studies have focused on the thermoplastic PI systems. [14–21], most of which were aimed at electronic packaging applications. All of the systems were condensation polymers, based on the condensation reaction of a dianhydride with a diamine. For example, Yano et al. [14] have studied PIs based on pyromellitic dianhydride (PMDA) and 4,4'-diaminophenyl ether in dimethylacetamide. They found that a several-fold reduction in permeability of small gases was achieved, despite having an intercalated morphology. A parallel study by Lan et al. [15] confirmed the findings of Yano et al. Also Chang et al. [16] reported a study of a thermoplastic PI nanocomposite based on PMDA and benzidine. They prepared nanocomposites using different organically modified montmorillonite and achieved significant improvements in tensile and barrier properties.

The durability and reliability of materials used in aerospace components is a critical concern. Among the

---

\* Corresponding author. Tel.: +1-334-727-4247; fax: +1-334-727-4224.  
E-mail address: deand@tusk.edu (D. Dean).

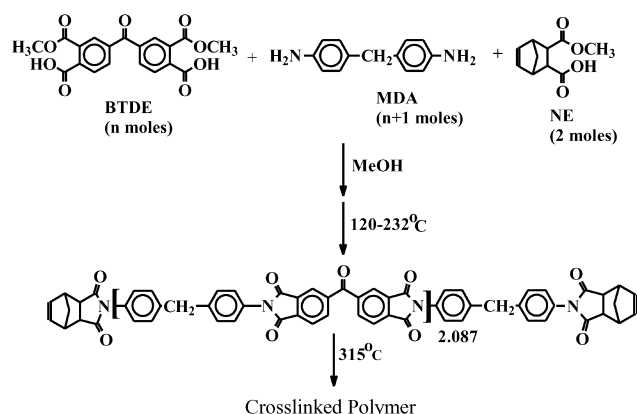


Fig. 1. Synthetic scheme for PMR-15.

materials requirements for these applications are a high glass transition temperature ( $T_g$ ), high temperature stability in a variety of environments, and good mechanical properties over a wide range of temperatures [22]. In this study, we have used a thermosetting, PMR-type PI, PMR-15, to synthesize a class of high temperature nanocomposites. Polymerization of monomer reactants (PMR)-type polyimides are thermosetting polymers which combine excellent processability, mechanical properties, and thermal oxidative stability (TOS). These materials are attractive for use in aerospace components where durability and reliability are critical concerns. Among the materials requirements for these applications are a high glass transition temperature ( $T_g$ ), high temperature stability in a variety of environments, and good mechanical properties over a wide range of temperatures [22]. In contrast to the PI's discussed above, PMR-15 is prepared in two stages, as shown in Fig. 1. PMR-15 synthesis involves three monomers: 2-carboxy-3-methoxy-5-norbornene (nadic ester, NE), 4,4'-methylenedianiline (MDA), and the dimethyl ester of 3,3',4,4'-benzophenonetetracarboxylic acid (BTDE). The oligomers formed from this reaction typically have a molecular weight of 1500, hence the name PMR-15. Curing under heat and pressure results in a highly crosslinked network structure [23]. There has been a significant amount of research aimed at increasing the TOS of PMR-15 by altering the structure of the dianhydride, [24] the diamine, [23,25,26] or the end-cap [27]. An alternative to modification of the polymer, as a means of increasing TOS, is the dispersion of a layered silicate in the polymer matrix [28, 29]. In this work, LS have been modified using a primary amine (dodecylamine: 12 carbons) and an amino acid (11-aminoundecanoic acid: 11 carbons). Modifiers with 10–12 carbons have been proven to be appropriate to render the hydrophilic LS to be dispersed in the organic solvents [14]. The carboxylic group in the amino acid is expected to give a better interaction between the polymer matrix and the OLS reinforcement. In this study, we will report the synthesis and morphological characterization of LS and OLS/PMR-15 nanocomposites as well as the viscoelastic and mechanical

properties of the consolidated nanocomposites versus those of the neat polyimide.

## 2. Experimental

### 2.1. Reagents

PGV (Nanacor) is a  $\text{Na}^+$ -montmorillonite with cation-exchange capacity (CEC) of 140 mequiv/100 g. PMR-15 polyimide precursor solution (72% solids in methanol) was obtained from HyComp, Inc. The modifiers, dodecylamine and 11-aminoundecanoic acid (Aldrich) were used as received.

### 2.2. Preparation of organically modified layered silicates

The OLS were synthesized by a cation-exchange reaction between the PGV and the ammonium salt of modifiers' (dodecylamine and 11-aminoundecanoic acid) [14]. PGV was dispersed in water at 70–80 °C. Excess modifier (twice the CEC of the clay) was dissolved in water at 70–80 °C and an equivalent amount of concentrated HCl acid was added to the solution. The dispersion of PGV was added to the solution of the modifier and this mixture was stirred vigorously for 1 h. A white precipitate was isolated by suction-filtration, placed in a 600 ml beaker with 400 ml of hot water, and stirred for 1 h. This process was repeated two times to ensure the removal of the excess ammonium salt. The filter cake was then freeze-dried overnight.

### 2.3. Preparation of polyimide-clay nanocomposites

A desired amount (10–15 g) of PMR-15 precursor solution and varying amounts (2.5 and 5 wt%) of PGV or OLS was added. Methanol (100–150 ml) was added for dilution. The mixture was stirred at room temperature for 1.5 h with a mechanical stirrer to perform dispersion of the clay into the polymer matrix. The methanol was evaporated off at 50–60 °C. A viscous solution of PMR-15/clay nanocomposite was obtained. The viscous nanocomposites solutions were imidized (or B-staged) at 204 °C (5.1 °C/min) for 1 h and 232 °C (1.4 °C/min) for 30 min. The imidized products were ground, to form a golden powder.

### 2.4. Consolidation of the nanocomposites

The B-staged powders were placed in a mold ( $4 \times 4 \times 0.039$  in.<sup>3</sup>) and a thermocouple of a digital thermometer was connected to the mold. The mold was placed in the Carver laboratory hydraulic press and heating started. Pressure (2000 psi) at 270 °C was applied and the mold was held at these conditions for 2 h. The heat was turned off and the mold was left to cool to room temperature before the molded samples were removed. The molded

samples were post-cured in an air-circulating oven at 315 °C for 5 h.

### 2.5. Characterization

Wide angle X-ray scattering measurements on crushed consolidated samples were performed using Philips XRG 3100 diffractometer with Cu  $K_{\alpha}$  ( $\lambda = 1.54 \text{ \AA}$ ) radiation. An accelerating voltage of 40 kV/170 mA was maintained. The step size and the scanning speed were 0.02° and 0.5 s/step, respectively. Transmission electron microscopy (TEM) specimens were prepared by microtoming sections of post-cured PMR-15 nanocomposites, 20–70 nm thick, and floating the sections onto Cu grids. Micrographs were obtained with a Philips CM 200, using an acceleration voltage of 200 kV.

Glass transition temperatures ( $T_g$ ), storage modulus and loss modulus were obtained using a Dynamic Mechanical Analyzer (TA Instruments DMA 2980). A sample geometry of 40 mm  $\times$  12.5 mm  $\times$  3 mm ( $L \times W \times T$ ), a frequency of 1 Hz, amplitude of 10  $\mu\text{m}$  and a scan rate of 5 °C/min was used. Coefficient of thermal expansion was determined using a Thermomechanical Analyzer (TA Instruments TMA 2940). Multiple scans were conducted to ensure reproducibility, but not enough to perform statistical analysis of the variations. Flexural properties were measured using an RSI Minimat materials tester. The tests were performed in the 3-point bending mode using crosshead speed of 0.5 mm/min using a span-to-depth ratio of 7:1. At least five samples were tested and the average along with the standard deviation was reported.

## 3. Results and discussions

### 3.1. Preparation of organically modified layered silicates

The modification of surface of the LS was done to achieve better interaction between the hydrophilic clay and the hydrophobic polymer. In this study, we used an ammonium salt of a primary amine, dodecylamine and an amino acid, 11-aminoundecanoic acid for exchanging of the  $\text{Na}^+$  ions on the LS surface. XRD curves of the LS and OLS are shown in Fig. 2. The peak observed for the LS (PGV) at  $2\theta = 6.63^\circ$  ( $d_{001} = 13.3 \text{ \AA}$ ), which corresponds to the basal spacing between the layers of the silicate layers, shifts to a lower angle. PGVC10COOH, modified 11-aminoundecanoic acid, exhibited a sharp intense peak at  $4.97^\circ$  corresponding to a  $d$ -spacing of 17.8  $\text{\AA}$ . While the PGVC12, modified using dodecylamine, exhibited a sharp intense peak at  $2\theta = 4.36^\circ$  corresponding to a  $d$ -spacing of 20.3  $\text{\AA}$ . Thus, in both modified PGV clays, the interlayer spacing has expanded signifying the incorporation of the modifiers between the silicate layers.

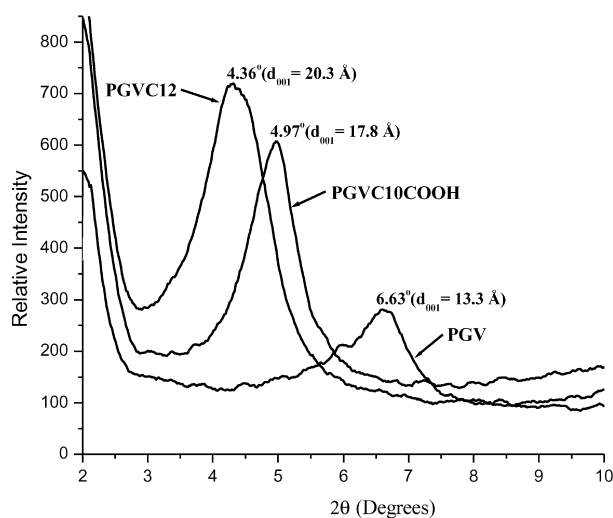


Fig. 2. XRD curves of PGV and organically modified PGV.

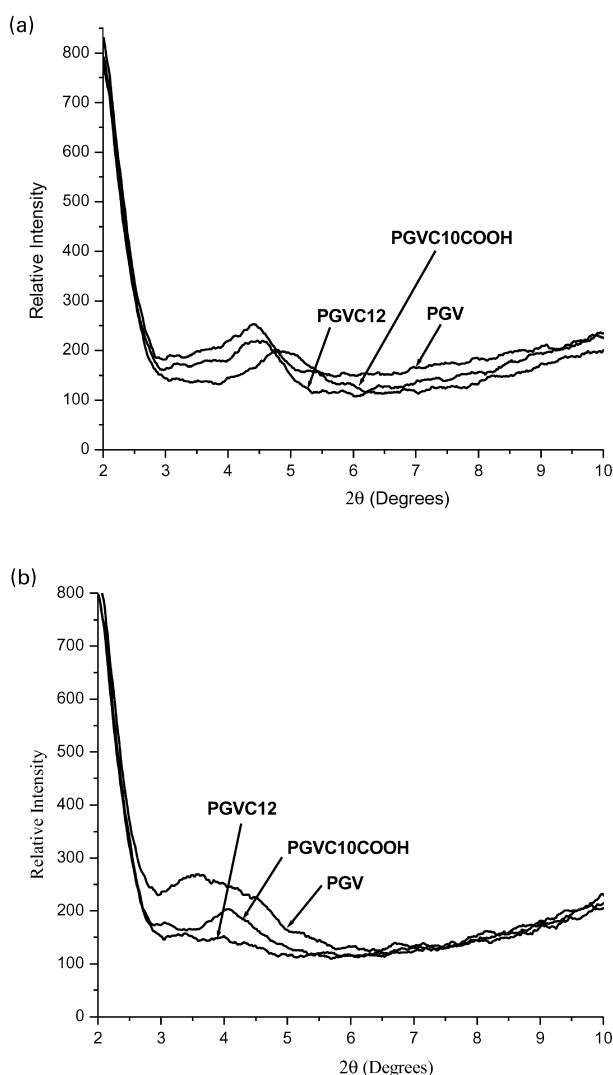


Fig. 3. (a) XRD curves of B-staged 2.5% clay loaded LS and OLS nanocomposites. (b) XRD curves of consolidated 2.5% clay loaded LS and OLS nanocomposites.

Table 1  
XRD analyses of 2.5% clay loaded nanocomposites

	PGV		PGVC10COOH		PGVC12	
	2θ (°)	d <sub>001</sub> (Å)	2θ (°)	d <sub>001</sub> (Å)	2θ (°)	d <sub>001</sub> (Å)
Unmodified clay	6.63	13.3	4.97	17.8	4.36	20.3
2.5% <sup>a</sup>	4.90	18.0	4.41	20.0	4.30	20.5
2.5% <sup>b</sup>	3.96	22.3	4.08	21.6	–	–

<sup>a</sup> B-staged.

<sup>b</sup> Consolidated.

### 3.2. X-ray diffraction analyses of PMR-15/LS and OLS nanocomposites

The development in the morphology of the nanocomposites prepared was studied by analyzing XRD curves of PGV, organically modified PGV, B-staged (imidized) and consolidated (fully cured) nanocomposites. XRD curves of

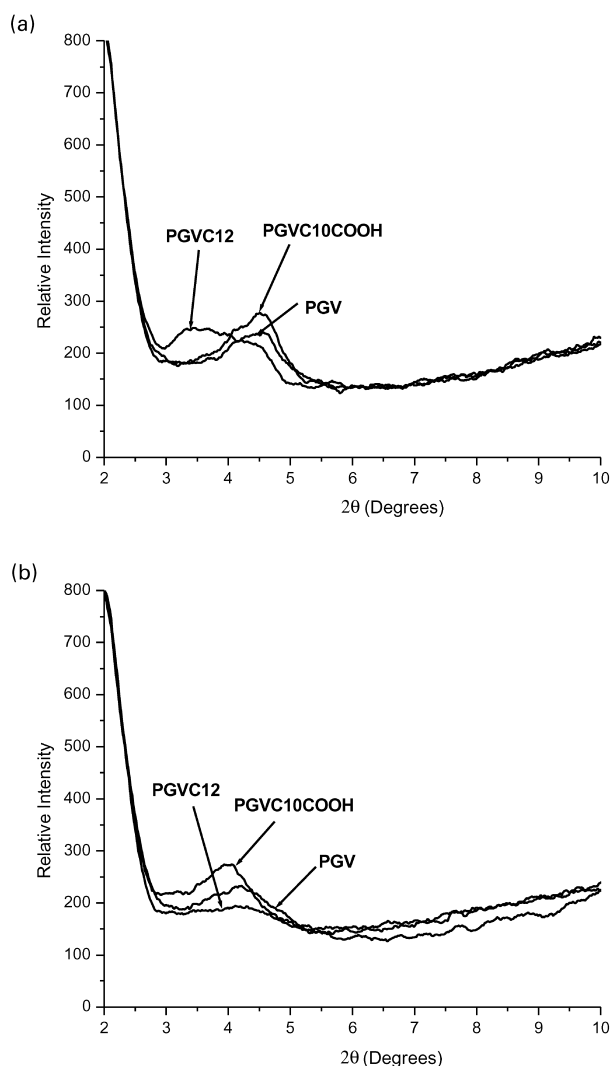


Fig. 4. (a) XRD curves of B-staged 5% clay loaded LS and OLS nanocomposites. (b) XRD curves of consolidated 5% clay loaded LS and OLS nanocomposites.

Table 2  
XRD analyses of 5% clay loaded nanocomposites

	PGV		PGVC10COOH		PGVC12	
	2θ (°)	d <sub>001</sub> (Å)	2θ (°)	d <sub>001</sub> (Å)	2θ (°)	d <sub>001</sub> (Å)
Unmodified clay	6.63	13.3	4.97	17.8	4.36	20.3
5% <sup>a</sup>	4.50	19.6	4.52	19.5	3.99	22.1
5% <sup>b</sup>	4.19	21.1	4.01	22.0	–	–

<sup>a</sup> B-staged.

<sup>b</sup> Consolidated.

the (a) B-staged and (b) consolidated (2.5% clay loading) nanocomposites are shown in Fig. 3. Table 1 summarizes the analyses of these XRD curves. The B-staged prepolymers exhibited weaker peaks that were shifted to lower angles compared to the organically modified PGVs, suggesting that the PMR-15 oligomers diffused and intercalated between the clay layers leading to partial disruption of the clay layers. The broadening of the peaks for the consolidated PGV and PGVC10COOH/PMR-15 nanocomposites indicated that further intercalation into the silicate clay layers has occurred, although complete exfoliation has not been achieved. It should be noted that the studies on PI-based nanocomposites cited earlier only used organically modified silicates. These studies all used NMP as the solvent, whereas our study used methanol, which is more polar and has a higher propensity to swell the unmodified PGV. The peak at  $2\theta = 4.43^\circ$  for the B-staged PGVC12/PMR-15 (2.5% clay loaded) nanocomposites totally disappears in the scan for the consolidated (fully cured) samples, indicative of a loss of ordering of the clay layers required to satisfy Bragg's condition for diffraction. A similar result is observed for PGVC12/PMR-15 (5% clay loaded), which is shown in Fig. 4 (and summarized in Table 2). This may possibly be due to orientation of the layers induced by the consolidation. TEM of the sample (Fig. 5) indicates that intercalated domains are still present in the

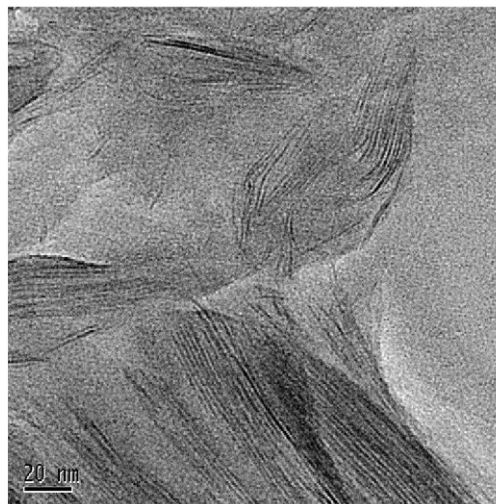


Fig. 5. TEM micrograph of PGVC12/PMR-15 (5% clay loaded).

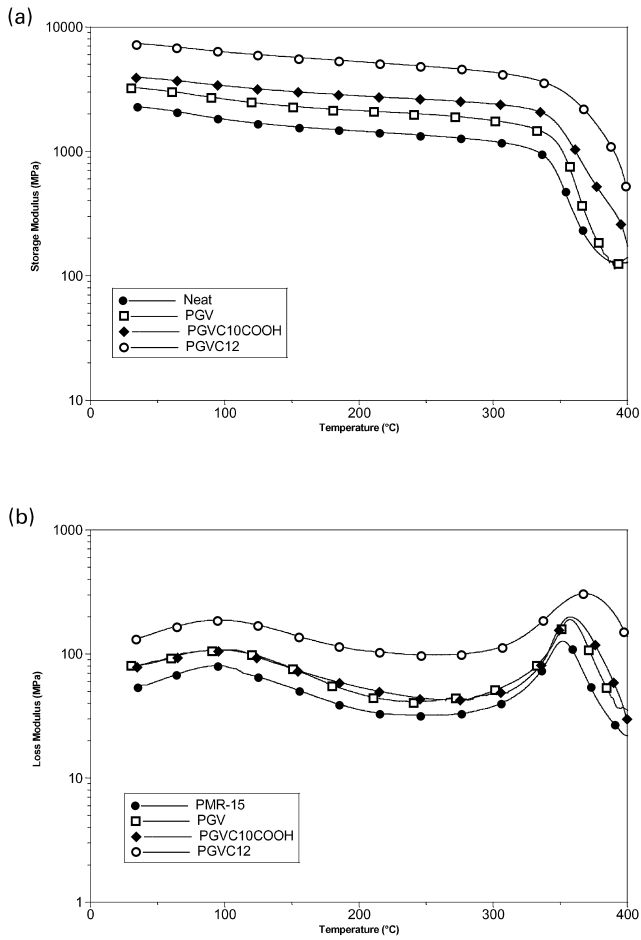


Fig. 6. (a) Storage modulus of neat PMR-15, LS and OLS/PMR-15 nanocomposites (2.5% clay loading). (b) Loss modulus of neat PMR-15, LS and OLS/PMR-15 nanocomposites (2.5% clay loading).

sample, however. The persistence of the intercalated morphology in the consolidated sample is presumably due to the inability of the prepolymer to diffuse into the layers and subsequently delaminate them during the crosslinking stage. This may be due to the relatively large size of the prepolymer. A potential approach to achieve an exfoliated morphology may be to disperse the clay in the monomeric mixture, before polyamic acid formation [18,19]. This will be investigated further.

### 3.3. Viscoelastic properties of PMR-15/LS and OLS nanocomposites

Dynamic mechanical analysis for the consolidated LS and OLS/PMR-15 nanocomposites was conducted to examine the effect of the clays on the thermomechanical properties of the polyimide nanocomposites. In Fig. 6, (a) the storage modulus ( $E'$ ) and (b) loss modulus ( $E''$ ) of the 2.5% clay loaded nanocomposite are shown. Addition of the clays increases the level of the  $E'$  in the glassy region, with the highest value observed for the PGVC12. The effect of the clays on the relaxation behavior and  $T_g$  can be seen by

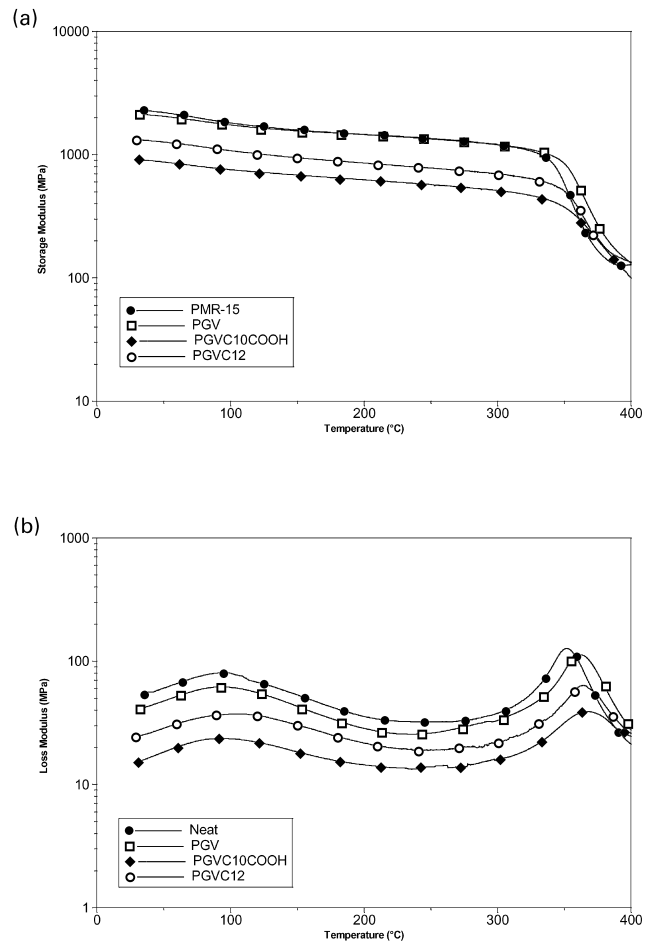


Fig. 7. (a) Storage modulus of neat PMR-15, LS and OLS/PMR-15 nanocomposites (5% clay loading). (b) Loss modulus of neat PMR-15, LS and OLS/PMR-15 nanocomposites (5% clay loading).

observing both the  $E'$  and  $E''$  curves. Both curves indicate an increase in the  $T_g$ , accompanied by a broadening of this relaxation indicative of restriction of segmental relaxation. The values for  $T_g$ s (which were measured from the  $E''$  curves) are summarized in Table 3. The average  $T_g$  increase was 9 °C, with the PGVC12/PMR-15 exhibiting a 16 °C increase. The  $E''$  curves also show a broad  $\beta$  relaxation centered near 100 °C, which has been attributed to crosslink motion in PMR-15. This relaxation becomes broader upon addition of clay, with the largest effect again observed for the PGVC12 clay. These results ( $T_g$  and  $\beta$  relaxation changes) indicate polymer–clay interaction at least at the segment level [30]. This effect is not observed for the samples containing 5% clay, however (Fig. 7). In fact, both

Table 3  
 $T_{g,s}$  (°C) of neat PMR-15, LS and OLS/PMR-15 nanocomposites

Clay loading (%)	PGV	PGVC12	PGVC10COOH
0	351	351	351
2.5	357	367	358
5	361	369	366

Table 4  
Flexural properties of neat PMR-15, LS, and OLS/PMR-15 nanocomposites

	Clay loading (%)	Modulus (GPa)	Strength (MPa)	Elongation at break (%)
Neat	0	3.5 ± 3%	96 ± 2%	2.6 ± 6
PGV	2.5	4.3 ± 2%	109 ± 3%	2.8 ± 5
	5	3.4 ± 3%	76 ± 4%	2.3 ± 3
PGVC10COOH	2.5	5.7 ± 4%	143 ± 4%	2.9 ± 6
	5	3.4 ± 1%	110 ± 3%	1.6 ± 5
PGVC12	2.5	4.6 ± 2%	97 ± 3%	1.5 ± 5
	5	2.9 ± 3%	57 ± 5%	2.0 ± 6

the samples containing organically modified clays have glassy  $E'$  values lower than that for PMR-15, while the PGV/PMR sample has an  $E'$  value equal to that of the PMR-15. The  $T_g$  has increased by an average of 14 °C for these systems. This finding is corroborated by the  $E''$  curve, which also shows little or no effect of the clays on the  $\beta$  relaxation.

#### 3.4. Flexural properties of PMR-15/LS and OLS nanocomposites

Table 4 summarize the flexural properties of the 2.5 and 5% clay loaded nanocomposites, respectively. For the neat PMR-15 polyimide, the flexural modulus was 3.5 GPa. With the incorporation of 2.5% PGV, the flexural modulus increased to 4.3 GPa, representing a 23% increase. The nanocomposites loaded with 2.5% of the OLS, PGVC10COOH and PGVC12, showed a 63 and 31%, respectively, increase in the modulus compared to the neat PMR-15. The increase in the flexural modulus and strength of the nanocomposites is accompanied by a small increase in the elongation at break (except for the PGVC12/PMR-15). As shown in Table 4, increasing the clay loading to 5% did not show a significant improvement in the flexural modulus, strength and elongation of the nanocomposites (except for the PGVC10COOH/PMR-15). In fact, a decrease was observed. This variation in the trend may be caused by variations in the clay–polymer interface caused by an unknown degree of modifier degradation, since these modifiers are known to exhibit degradation onsets well below the PMR-15 crosslinking temperature of 316 °C [28, 29,31]. The morphological heterogeneity of the intercalated morphology is also a primary contributor [12]. It has been suggested that a more homogeneous, exfoliated morphology would exhibit even better properties [12]. Examination of the flexural strength at clay loading of 2.5% reveals a 14 and 49% increase for the PGV and PGVC10COOH, respectively, while no change is observed for the PGVC12 sample. The enhanced properties for the PGVC10COOH relative to the PGVC12 sample are assumed to be due to the more favorable interaction between the carboxylic acid functional groups of the modifier and the polymer [32].

#### 3.5. Linear coefficient of thermal expansion of PMR-15/LS and OLS nanocomposites

Table 5 shows the coefficients of thermal expansion (CTE) of the neat PMR-15 and the LS and OLS nanocomposites. It was found that the CTE decreased only for the PGV/PMR-15 nanocomposite while it increased in the case of the OLS/PMR-15 nanocomposites. A similar trend has been reported for thermoplastic polyimide nanocomposites [17]. As stated in Section 3.4, potential variations in the interface and the heterogeneous morphology could possibly lead to the increases in the CTEs of the OLS/PMR-15 nanocomposites that are observed.

## 4. Conclusions

High temperature, thermoset PMR-15/LS and OLS nanocomposites have been prepared using conventional organically modified clays as well as an unmodified clay. The methanol solvent has a propensity to swell the unmodified clay, resulting in nanocomposite formation, without the use of a modifier. Structural evolution as a function of curing has been studied using XRD and TEM. The persistence of the intercalated morphologies even after consolidation and crosslinking, is presumed to arise because of the inability of more of the relatively large prepolymer to diffuse into the interlayers before gelation and vitrification occurred. Incorporation of 2.5% clay showed a significant improvement in the flexural modulus and strength with no reduction in the elongation. Doubling the clay loading percentage resulted in degradation of the nanocomposite flexural properties. Higher  $T_g$ s were measured for all the nanocomposite compared to the neat PMR-15, with the

Table 5  
CTEs ( $\mu\text{m}/^\circ\text{C}$ ) of the neat PMR-15, LS and OLS/PMR-15 nanocomposites

Clay loading (%)	PGV	PGVC10COOH	PGVC12
0	46.3	46.3	46.3
2.5	34.4	53.0	49.8
5	38.6	56.2	58.5

highest values obtained for the 5% clay loaded samples. The effect of the LS on the relaxation behavior (i.e.  $T_g$  enhancements and broadening of  $\beta$  relaxation) indicated polymer–clay interaction at the segmental level. An improvement in the CTE was observed for the PGV/PMR-15 nanocomposites, while a decrease was observed for the organically modified samples. This was attributed to potential variations in the interface caused by modifier degradation. While a slight, although unknown amount of modifier degradation is possible for the modified silicates during the crosslinking step, significant improvements in the  $T_g$ s and mechanical properties were obtained for relatively low clay loadings. Thus, the nanocomposite approach seems to hold promise as a way to enhance the properties of this high performance polymer.

### Acknowledgments

The authors would like to thank David Hull (GRC) for TEM analysis and Ralph Garlick (GRC) for XRD analysis. This work was funded by National Aeronautics and Space Administration (Grant no. NAG3-2432).

### References

- [1] Usuki A, Kawasumi M, Kojima Y, Okada A, Kurauchi T, Kamigaito O. *J Mater Res* 1993;8:1174.
- [2] Usuki A, Kojima Y, Kawasumi M, Okada A, Fukushima Y, Kurauchi T, Kamigaito O. *J Mater Res* 1993;8:1179.
- [3] Kojima Y, Usuki A, Kawasumi M, Okada A, Fukushima Y, Kurauchi T, Kamigaito O. *J Mater Res* 1993;8:1185.
- [4] Kojima Y, Usuki A, Kawasumi M, Okada A, Fukushima Y, Kurauchi T, Kamigaito O. *J Polym Sci, Part A: Polym Chem* 1993;31:983.
- [5] Giannelis EP. *J Miner Met Mater Soc* 1992;March:28.
- [6] Okada A, Usuki A. *Mater Sci Engng* 1995;C3:109.
- [7] Giannelis EP. *J Adv Mater* 1996;8:29.
- [8] Ogawa M, Kuroda K. *Bull Chem Soc Jpn* 1997;70:2593.
- [9] Messersmith PB, Giannelis EP. *J Polym Sci, Part A: Polym Chem* 1995;33:1047.
- [10] Messersmith PB, Giannelis EP. *Chem Mater* 1994;6:1719.
- [11] Lan T, Kaviratna PD, Pinnavaia TJ. *Chem Mater* 1995;7:2144.
- [12] Le Baron P, Wang Z, Pinnavaia T. *Appl Clay Sci* 1999;15:11.
- [13] Giannelis EP. *Adv Mater* 1996;8:29.
- [14] Yano K, Usuki A, Okada A, Kurauchi T, Kamigaito O. *J Polym Sci, Part A: Polym Chem* 1993;31:2493.
- [15] Lan T, Kaviratna P, Pinnavaia T. *Chem Mater* 1997;6:573–5.
- [16] Chang JH, Park K, Cho D, Yang H, Ihn K. *Polym Engng Sci* 2001;41(9):1514.
- [17] Hsiao S, Liou G, Chang L. *J Appl Polym Sci* 2001;80(11):2067–72.
- [18] Delozier D, Orwoll R, Cahoon J, Johnston N, Smith J, Connell J. *Polymer* 2002;43:813–22.
- [19] Magaraphan R, Lilayuthalart W, Sirivat A, Schwank J. *Compos Sci Technol* 2001;61:1253–64.
- [20] Kim J, Ahmed R, Lee S. *J Appl Polym Sci* 2001;80:592–603.
- [21] Tyan H, Wei K, Hsieh T. *J Polym Sci, Part B: Polym Phys* 2000;22:2873–8.
- [22] Meador M. *Ann Rev Mater Sci* 1998;28:599.
- [23] Delvigs P, Klopotek DL, Cavano PJ. *High Perform Polym* 1994;6:209.
- [24] Alston W. *High Perform Polym* 1995;7(1):93.
- [25] Delvigs P, Klopotek DL, Cavano PJ. *High Perform Polym* 1997;9:161.
- [26] Chuang K, Waters J, Hardy-Green D. 42nd Int SAMPE Symp 1997;42:1283.
- [27] Meador M. *Chem Mater* 2001; ASAP Article.
- [28] Islam M, Dean D, Campbell S. *Am Chem Soc, Polym Sci Engng* 2001;84.
- [29] Campbell S, Scheiman D, Faile M, Papadopoulos D. In preparation.
- [30] Utracki LA. *Polymer alloys and blends: thermodynamics and rheology*. New York: Hanser; 1990.
- [31] Xie W, Goa Z, Pan W, Hunter D, Singh A, Vaia R. *Chem Mater* 2001;13:2979–90.
- [32] Agag T, Koga T, Takeichi T. *Polymer* 2001;42:3399–408.